Maximum loads for eccentrically loaded thin-walled channel struts

Autor(en): **Walker, A.C.**

Objekttyp: **Article**

Zeitschrift: **IABSE publications = Mémoires AIPC = IVBH Abhandlungen**

Band (Jahr): **28 (1968)**

PDF erstellt am: **16.08.2024**

Persistenter Link: https://doi.org/10.5169/seals-22188

Nutzungsbedingungen

Die ETH-Bibliothek ist Anbieterin der digitalisierten Zeitschriften. Sie besitzt keine Urheberrechte an den Inhalten der Zeitschriften. Die Rechte liegen in der Regel bei den Herausgebern.
Die auf der Plattform e-periodica veröffentlichten Dokumente stehen für nicht-kommerzielle Zwecke in Lehre und Forschung sowie für die private Nutzung frei zur Verfügung. Einzelne Dateien oder Ausdrucke aus diesem Angebot können zusammen mit diesen Nutzungsbedingungen und den korrekten Herkunftsbezeichnungen weitergegeben werden.
Das Veröffentlichen von Bildern in Print- und Online-Publikationen ist nur mit vorheriger Genehmigung der Rechteinhaber erlaubt. Die systematische Speicherung von Teilen des elektronischen Angebots auf anderen Servern bedarf ebenfalls des schriftlichen Einverständnisses der Rechteinhaber.

Haftungsausschluss

Alle Angaben erfolgen ohne Gewähr für Vollständigkeit oder Richtigkeit. Es wird keine Haftung übernommen für Schäden durch die Verwendung von Informationen aus diesem Online-Angebot oder durch das Fehlen von Informationen. Dies gilt auch für Inhalte Dritter, die über dieses Angebot zugänglich sind.

Ein Dienst der *ETH-Bibliothek*
ETH Zürich, Rämistrasse 101, 8092 Zürich, Schweiz, www.library.ethz.ch

http://www.e-periodica.ch

Maximum Loads for Eccentrically Loaded Thin-walled Channel Struts

Charges maximales pour piles à parois minces en U, comprimées excentriquement

Höchstlasten für dünnwandige U-Stützen unter ausmittiger Belastung

A. C. WALKER
Department of Civil Engineering, University College, London

Introduction

The use of thin-walled open sections as load-bearing members in civil engineering structures has increased considerably in the last few years. This has given rise to a greater need to understand the mechanics of the behaviour of these sections and also to obtain design information in a simple and comprehensible manner. Although considerable research effort [1–3] has been applied to the testing and analysis of uniformly-compressed channel-columns, relatively little attention has been given to the more general condition in which the load is applied offset from the centroid of the cross-section. This paper reports on work carried out on this problem both from an experimental and theoretical standpoint.

The paper is concerned with channel columns having one axis of symmetry in the cross-section, and in the analysis it is assumed that the compressive

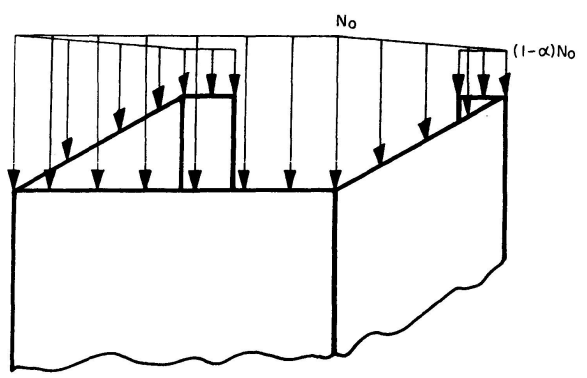

Fig. 1. Channel loading geometry.

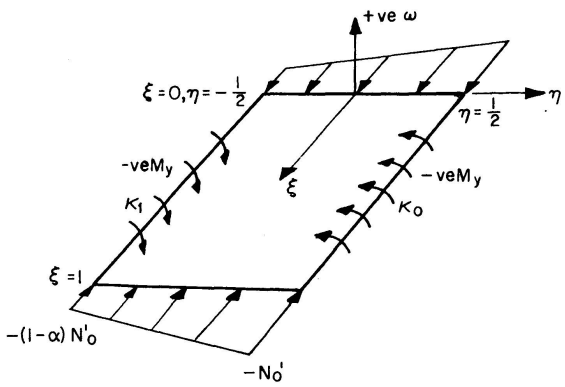

Fig. 2. Non-dimensional representation of plate geometry edge-loading and edge restraints.

load is applied along this axis; then the web of the channel is compressed uniformly, while a linearly varying stress is applied to the flanges, as in Fig. 2. It is also assumed that open thin-walled channel-sections, in which the length is of the same order of magnitude as the flange or web widths, may be considered from a theoretical viewpoint to be composed of individual plates that are connected in a certain manner on their common longitudinal edges. The determination of the channel load-bearing characteristics then becomes one of obtaining the corresponding plate properties and combining these to obtain compatible conditions along the adjoining edge.

We first consider the behaviour of thin, initially flat, plates loaded by a linearly varying edge stress. It has been shown [4] that such plates may sustain load considerably in excess of the theoretical buckling loads before collapse occurs. Also, good engineering estimates of these maximum loads may be obtained analytically by assuming that collapse takes place when the direct stress at the edge reaches the material compressive yield stress. Since the unloaded edge conditions were taken to be rotationally restrained the calculated plate instability loads may be synthesise to provide the theoretical buckling loads [5] of open sections considered to be composed of such plates. In practice, no plate is perfectly flat, and deflections will grow from the beginning of load application; for this reason, the theoretically predicted buckling behaviour is never experienced in practice. However, such a buckling analysis will indicate to a designer the loads for maximum growth of deformation and maximum rate of decrease of stiffness. Like their constituitive plates, compressed sections may sustain loads in excess of the theoretical buckling loads. In this paper an approximate method of analysis is presented which combines the plate collapse estimates to give the corresponding estimate for lipped sections. Test results are described which show that the estimates are good; these results are used as a basis for an empirical approach, by which the actual collapse loads may be predicted from the corresponding theoretical instability loads.

1. Analysis of Single Plates

a) Mathematical Formulation

Ref. [4] presents fully the analysis of the buckling and post-buckling behaviour of initially-flat, rectangular plates compressed by a linear-varying load action. The loaded edges were taken to be simply-supported whilst the longitudinal edges have equal or unequal rotational restraint; this is shown in Fg. 2. For the sake of completeness the above analysis is summarised in this paper. We put,

$$\xi = \frac{x}{a}, \quad \eta = \frac{y}{b}, \quad \phi = \frac{a}{b}, \quad \omega = \frac{w}{t}, \quad F' = \frac{F}{E\,t^2}, \tag{1}$$

where a is the length of the plate in the x direction and b is the breadth in the y direction; the VON KÁRMÁN [6] large deflection equations may be written in the nondimensional forms

$$\frac{1}{\phi^2}\frac{\partial^4\omega}{\partial\xi^4}+2\frac{\partial^4\omega}{\partial\xi^2\partial\eta^2}+\phi^2\frac{\partial^4\omega}{\partial\eta^4}=12(1-\nu^2)\left(\frac{\partial^2 F'}{\partial\xi^2}\frac{\partial^2\omega}{\partial\eta^2}+\frac{\partial^2 F'}{\partial\eta^2}\frac{\partial^2\omega}{\partial\xi^2}-2\frac{\partial^2 F'}{\partial\xi\,\partial\eta}\frac{\partial^2\omega}{\partial\xi\,\partial\eta}\right), \tag{2a}$$

$$\frac{1}{\phi^2}\frac{\partial^4 F'}{\partial\xi^4}+2\frac{\partial^4 F'}{\partial\xi^2\partial\eta^2}+\phi^2\frac{\partial^4 F'}{\partial\eta^4}=\left(\frac{\partial^2\omega}{\partial\xi\,\partial\eta}\right)+\frac{\partial^2\omega}{\partial\xi^2}\frac{\partial^2\omega}{\partial\eta^2}, \tag{2b}$$

where F' is the non-dimensional form of the Airy stress function, which is related to the direct and shear stresses by

$$\sigma_\xi=\frac{\sigma_x a^2}{\phi^2 E t^2}=\frac{\partial^2 F'}{\partial\eta^2},\qquad \sigma_\eta=\frac{\sigma_y a^2}{E t^2}=\frac{\partial^2 F'}{\partial\xi^2},\qquad \tau_{\xi\eta}=\frac{\tau_{xy} a^2}{\phi E t^2}=-\frac{\partial^2 F'}{\partial\xi\,\partial\eta}.$$

The in-plane boundary conditions for the loaded edges, $\xi=0$ and $\xi=1$, with the imposed loading and for zero shearing stress, are

$$[\sigma_\xi]_{\xi=0,1}=\left[\frac{\partial^2 F'}{\partial\eta^2}\right]_{\xi=0,1}=N_0'\left[\left(1-\frac{\alpha}{2}\right)+\alpha\eta\right], \tag{3a}$$

$$[\tau_{\xi\eta}]_{\xi=0,1}=\left[-\frac{\partial^2 F'}{\partial\xi\,\partial\eta}\right]_{\xi=0,1}=0, \tag{3b}$$

where $N_0'=\frac{N_0 a^2}{\phi^2 E t^3}$ and α is the eccentricity parameter.

Along the unloaded edges there is considered to be no direct stress acting in the η direction nor any shearing stress, so that

$$[\sigma_\eta]_{\eta=+1/2,-1/2}=\left[\frac{\partial^2 F'}{\partial\xi^2}\right]_{\eta=+1/2,-1/2}=0, \tag{4a}$$

$$[\tau_{\eta\xi}]_{\eta=+1/2,-1/2}=\left[\frac{\partial^2 F'}{\partial\xi\,\partial\eta}\right]_{\eta=+1/2,-1/2}=0. \tag{4b}$$

The out-of-plane boundary conditions along the loaded edges were those of simple support, i.e. if M_ξ is the linear intensity of bending moment about an axis parallel to the η axis, then

$$[M_\xi]_{\xi=0,1}=\left[\frac{\partial^2\omega}{\partial\xi^2}+\nu\phi^2\frac{\partial^2\omega}{\partial\phi^2}\right]_{\xi=0,1}=0, \tag{5a}$$

$$[\omega]_{\xi=0,1}=0. \tag{5b}$$

The unloaded edges are fully restrained against lateral deflection and elastically restrained against rotation, i.e.

$$[\omega]_{\eta=+1/2,-1/2} = 0, \tag{6a}$$

$$\left[\frac{\partial^2 \omega}{\partial \eta^2} + \frac{\nu}{\phi^2}\frac{\partial^2 \omega}{\partial \xi^2} - \kappa_1 \frac{\partial \omega}{\partial \eta}\right]_{\eta=+1/2,-1/2} = 0, \tag{6b}$$

$$\left[\frac{\partial^2 \omega}{\partial \eta^2} + \frac{\nu}{\phi^2}\frac{\partial^2 \omega}{\partial \xi^2} + \kappa_0 \frac{\partial \omega}{\partial \eta}\right]_{\eta=+1/2} = 0, \tag{6c}$$

where $\kappa_1 = -b\,r_1/D$, $\kappa_0 = -b\,r_0/D$ and r_1, r_0 are the degrees of rotation restraint.

An approximate solution of Eq. (2), together with the appropriate boundary conditions (Eq. (3–6)), is obtained using Galerkin's method and employing a digital computer to perform the necessary arithmetic. The trial series for F' is

$$F' = A\left[\left(1-\frac{\alpha}{2}\right)+\frac{\alpha}{3}\eta\right]\eta^2 + \sum_r \sum_s b_{rs} f_r(\xi)\, g_s(\eta), \tag{7}$$

where A is a constant, b_{rs} are constant coefficients, $f_r(\xi)$ and $g_s(\eta)$ are functions of ξ and η only, respectively. After consideration if Eqs. (3) and (4), Eq. (7) besomes

$$F' = \frac{N_0'}{2}\left[\left(1-\frac{\alpha}{2}\right)+\frac{\alpha}{3}\eta\right]\eta^2 + \sum_{r=1,2,\ldots}\ \sum_{s=0,1,\ldots} b_{rs}\sin^2 r\pi\xi\left(\eta^{s+4}-\frac{1}{2}\eta^{s+2}+\frac{1}{16}\eta^s\right). \tag{8}$$

Similarly a trial series for ω may be obtained which satisfies the appropriate boundary conditions (Eqs. (5) and (6)). This series may be written

$$\omega = \sum_{m=1,2,\ldots}\ \sum_{n=0,1,\ldots} q_{mn}\sin m\pi\xi\,[\eta^{n+4}+A_n\eta^{n+3}+B_n\eta^{n+2}+C_n\eta^{n+1}+D_n\eta^n], \tag{9}$$

where the coefficients A_n, B_n, etc., may be obtained from the solution of the matrix equation

$$\begin{bmatrix} 1 & 2 & 4 & 8 \\ 1 & -2 & 4 & -8 \\ 2(n+3)\left[(n+2)+\frac{\kappa_0}{2}\right] & 4(n+2)\left[(n+1)+\frac{\kappa_0}{2}\right] & 8(n+1)\left[n+\frac{\kappa_0}{2}\right] & 16n\left[(n-1)+\frac{\kappa_0}{2}\right] \\ 2(n+3)\left[(n+2)+\frac{\kappa_1}{2}\right] & -4(n+2)\left[(n+1)+\frac{\kappa_1}{2}\right] & 8(n+1)\left[n+\frac{\kappa_1}{2}\right] & -16n\left[(n-1)+\frac{\kappa_1}{2}\right] \end{bmatrix} \cdot \begin{bmatrix} A_n \\ B_n \\ C_n \\ D_n \end{bmatrix} = \begin{bmatrix} -\frac{1}{2} \\ \frac{1}{2} \\ -(n+4)\left[(n+3)+\frac{\kappa_0}{2}\right] \\ (n+4)\left[(n+3)+\frac{\kappa_1}{2}\right] \end{bmatrix}.$$

b) Buckling

Theoretically buckling occurs when the flat plate becomes unstable at a particular value of the applied stress distribution. Thus, in Eq. (8) we have

$b_{rs} \equiv 0$, and, if the plate is considered to buckle in a unique sinewave form in the longitudinal direction, we may write Eq. (9) in the form

$$\omega = \sum_{n=0,1,\ldots}^{n=L} q_n \sin m\pi\xi\, Y_n, \tag{10}$$

where $$Y_n = [\eta^{n+4} + A_n \eta^{n+3} + B_n \eta^{n+2} + C_n \eta^{n+1} + D_n \eta^n].$$

Thus Galerkin's method when applied to Eq. (2) using $b_{rs} = 0$ and Eq. (10), gives

$$\sum_{n=0,1,\ldots}^{n=L} q_n \int_{-1/2}^{1/2} \left\{ \frac{d^4 Y_n}{d\eta^4} - 2\frac{m^2\pi^2}{\phi^2}\frac{d^2 Y_n}{d\eta^2} + \frac{m^4\pi^4}{\phi^4} Y_n - k\frac{m^2\pi^2}{\phi^2}\left[\left(1-\frac{\alpha}{2}\right) + \alpha\eta\right] Y_n \right\} Y_j\, d\eta = 0 \qquad (0 \leqq j \leqq L), \tag{11}$$

where $$k = -\frac{N_0 b^2}{D}.$$

Evaluation of Eq. (11) leads to an algebraic eigenvalue problem for k, the buckling coefficient. This is very easily programmed for solution on a digital computer, and it has been shown [5] that the buckling coefficient converges rapidly for increasing number of terms (L). The buckling load is obtained from

$$P_{crit.} = -\frac{kD}{b}\left(1-\frac{\alpha}{2}\right).$$

c) Post-buckling Behaviour

It is assumed here that there is no change of buckle pattern as the load is increased beyond the buckling load. Thus, if Eq. (9) is written

$$\omega = \sin m\pi\xi \sum_{n=0,1,\ldots}^{n=L} q_n [\eta^{n+4} + A_n \eta^{n+3} + B_n \eta^{n+2} + C_n \eta^{n+1} + D_n \eta^n],$$

and, if in Eq. (8) the summations are given the limits $1 \leqq r \leqq T$, $0 \leqq s \leqq u$, then Galerkin's method for Eq. (2) gives

$$\sum_{n=0,1,\ldots}^{n=L} \sum_{r=1,2,\ldots}^{r=T} \sum_{s=0,1,\ldots}^{s=U} \int_0^1 \int_{-1/2}^{1/2} \left[\frac{1}{\phi^2}\frac{\partial^4 F'}{\partial\xi^4} + 2\frac{\partial^4 F'}{\partial\xi^2\partial\eta^2} + \phi^2\frac{\partial^4 F'}{\partial\eta^4} - \left(\frac{\partial^2\omega}{\partial\xi\,\partial\eta}\right)^2 + \frac{\partial^2\omega}{\partial\xi^2}\frac{\partial^2\omega}{\partial\eta^2}\right] \frac{dF_{pq}}{db_{pq}}\, d\eta\, d\xi = 0, \tag{12a}$$

$$\sum_{n=0,1,\ldots}^{n=L} \sum_{r=1,2,\ldots}^{r=T} \sum_{s=0,1,\ldots}^{s=U} \int_0^1 \int_{-1/2}^{1/2} \left\{ \frac{1}{\phi^2}\frac{\partial^4\omega}{\partial\xi^4} + 2\frac{\partial^4\omega}{\partial\xi^2\partial\eta^2} + \phi^2\frac{\partial^4\omega}{\partial\eta^4} - 12(1-\nu^2)\left[\frac{\partial^2 F'}{d\xi^2}\frac{\partial^2\omega}{\partial\eta^2} + \frac{\partial^2 F'}{\partial\eta^2}\frac{\partial^2\omega}{\partial\xi^2} - 2\frac{\partial^2 F'}{\partial\xi\,\partial\eta}\frac{\partial^2\omega}{\partial\xi\,\partial\eta}\right]\right\} \frac{d\omega_i}{dq_i}\, d\eta\, d\xi = 0, \tag{12b}$$

where

$$1 \leqq p \leqq T, \quad 0 \leqq q \leqq U, \quad 0 \leqq i \leqq L.$$

Evaluation of Eq. (12) gives

$$[A]\,[b_{rs}] = [B]\,[q_i\, q_j], \tag{13}$$

$$\{[C_1'] - N_0'\,[C_2]\}\,[q_k] = [D]\,[b_{rs}\, q_k], \quad (0 \leqq i, j, k \leqq L) \tag{14}$$

where the coefficients of the matrices $[A], [B]$ etc., are constants. Substitution of $[b_{rs}]$, from Eq. (13) into Eq. (14), gives the simultaneous cubic equations

$$\{[C_1] - N_0'\,[C_2]\}\,[q_k] = [D']\,[q_i\, q_j\, q_k]. \tag{15}$$

This system of equations is solved by successive approximation on a digital computer for various values of $N_0' > N_{0\,crit.}'$

One result of this approximate solution is shown in Fig. 3; the direct longitudinal stress at the cross-section corresponding to the crest of a buckle

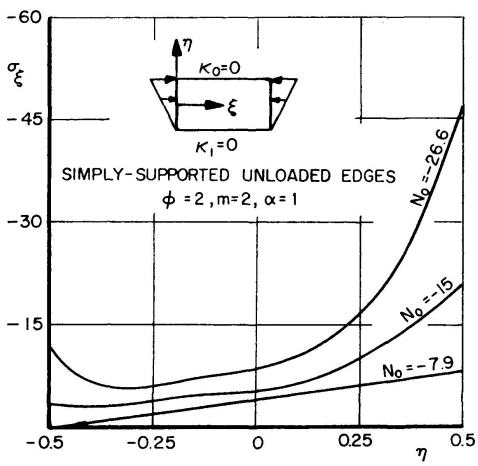

Fig. 3. Middle surface direct longitudinal stress at the crest of a buckle.

is plotted for various values of N_0'. It is seen that the stresses at the edges grow more rapidly than those in the middle, and this gives rise to the formulation of the collapse criterion. Results of tests given in Ref. [4] show that good agreement is obtained using the above analysis for buckling and maximum loads.

2. Collapse Loads for Channel Struts Reinforced with "Lips"

Fig. 4 shows how the section is considered to be subdivided into its constituent plates. The web is thus treated as a uniformly-loaded plate with equal amounts of rotational restraint along the unloaded edge. The flanges are taken to be eccentrically loaded plates elastically restrained against rotation along the unloaded edge common to itself and the web; the lip along the other unloaded edge is assumed to provide a simple support type of condition [7]. The matching at the common longitudinal edges is required to fulfill the following conditions.

a) The degree of edge restraint, r, for the flange and web is equal but opposite in sign, i.e. moment reactions are equal and the original corner geometry is maintained.
b) The value and distribution of the longitudinal direct stress, and therefore the unit shortening, were to be the same for the flange and web.

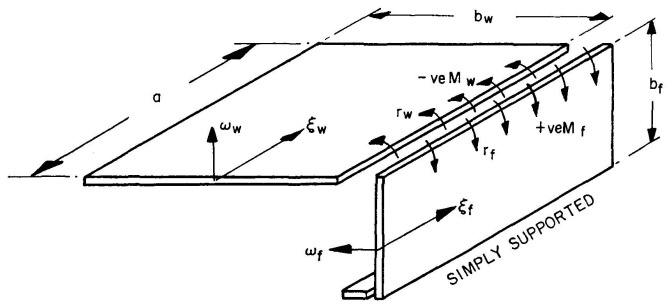

Fig. 4. Geometry and edge restraint representation of component plates of a lipped channel.

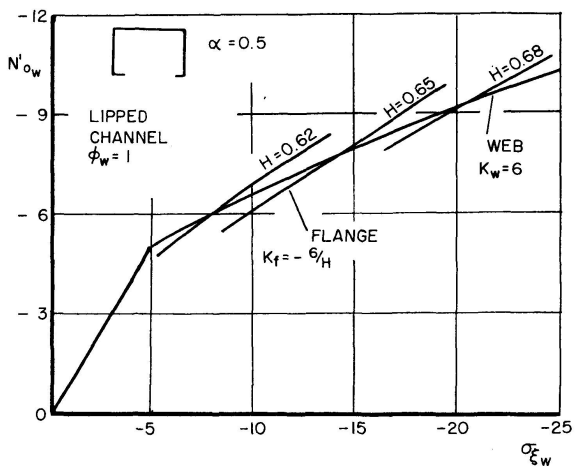

Fig. 5. Variation of load with longitudinal direct stress at $\eta = \frac{1}{2}$.

The simultaneous application of these requirements results in a very complex problem. This is simplified by assuming the stress distribution to be defined to sufficient accuracy by taking only one term in the ξ direction in the series Eq. (8). Now, taking a specific web geometry (ϕ_w, κ_w) we may, from the solution of the appropriate non-linear Eq. (15), obtain a plot of non-dimensionalised maximum edge stress against non-dimensional load parameter, as shown in fig. 5. Now

$$\kappa_w = -\frac{b_w r_w}{D_w} \quad \text{and} \quad \kappa_f = -\frac{b_f r_f}{D_f},$$

but by assumption, above we have, $r_f = -r_w$, and since we are considering only sections with uniform thickness, $D_f = D_w$. Thus, with $H = b_f/b_w$ we have

$$\kappa_f = \frac{b_w r_w}{D_w} \frac{b_f}{b_w} = -H \kappa_w.$$

Similarly, $\phi_f = 1/H \phi_w$, so that we may obtain corresponding plots on Fig. 5 for various values of H, and by using

$$\sigma_{\xi_w} = \frac{1}{H^2}\sigma_{\xi_f} \quad \text{and} \quad N'_{0_w} = \frac{1}{H^2}N'_{0_f},$$

they may be superposed on to the web plot as shown in Fig. 5. The intersections of these curves are valid geometries in that all the specified boundary matching conditions are fulfilled at the particular intersection load. Now, these particular geometries are considered to be sections at the point of collapse, i.e. the maximum direct longitudinal stress is equal to the material yield stress. Thus, using $\sigma_{xw} = \sigma_y$, where $\sigma_{xw} = \sigma_{\xi w}\phi_w^2 E h^2/a^2$, and prescribing a value for σ_y, we can obtain the thickness for the sections.

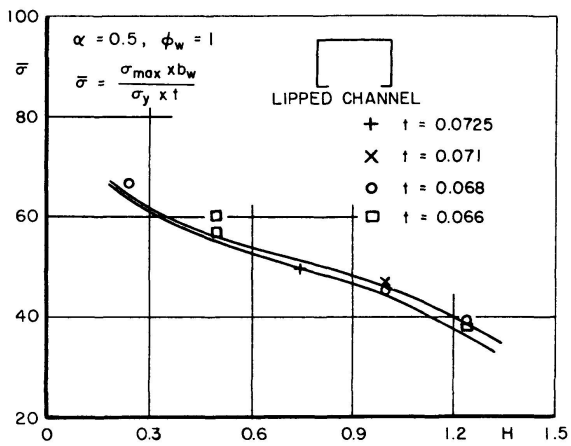

Fig. 6. Variation of non-dimensional maximum stress with shape factor $\alpha = 0.5$.

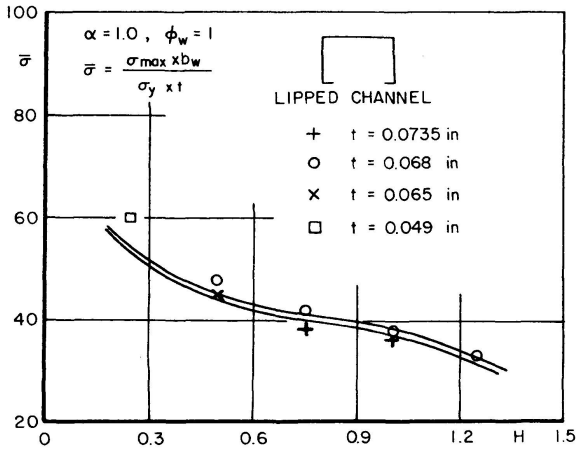

Fig. 7. Variation of non-dimensional maximum stress with shape factor $\alpha = 1.0$.

In this study, $\sigma_y = -35 \times 10^3$ lb. f/in^2, $\phi_w = 1$, $E = 33 \times 10^6$ lb. f/in^2, $a = 8$ in, and by limiting the thickness range to 0.050 in $-$ 0.090 in in the plots of collapse load against section geometry shown in Figs. 6 and 7 were calculated; in these, $\sigma = \frac{\sigma_{max} b_w}{\sigma_y h}$ and the lip width is 1 in. The procedure is shown in the following example, with

$$H = 0.62, \qquad \sigma_{\xi_w} = -8.35, \qquad N'_{0_w} = -6.02.$$

$$h = \left[\frac{\sigma_{x_w} a^2}{\phi_w^2 E\, \sigma_{\xi_w}}\right]^{1/2} = \left[\frac{-35 \times 10^3 \times 64}{1 \times 33 \times 10^6 \times -8.35}\right]^{1/2} = 0.0902 \text{ in.},$$

$$P_{max} = \frac{N'_0 h^3 E\, b_w (1 + 1.5\, H + 0.125)}{b_w^2} = 3.75 \times 10^3 \text{ tbf.},$$

$$\bar{\sigma} = \frac{\sigma_{max}}{\sigma_y}\frac{b_w}{h} = 52.9.$$

Similarly, with $H = 0.65$, $h = 0.0705$, $\sigma = 52.0$,
$H = 0.68$, $h = 0.0582$, $\sigma = 51.7$.

In this way Figs. 6 and 7 were constructed; due to the approximate nature of the solution of the plate differential equations there is some scatter in the theoretical results; this is contained in the enclosed area shown in these plots.

The most common design curve is that which enables the designer to calculate the maximum load for a section from the corresponding theoretical buckling load. Examples of this type of curve are given in Ref. [1] and [2] for uniformly compressed sections. The usefulness of this curve lies in the fact that the buckling load is relatively simple to calculate for even complex

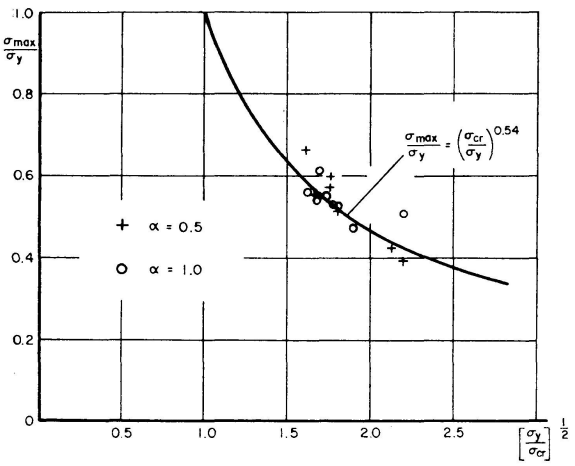

Fig. 8. Maximum strength of eccentrically loaded short lipped channel struts.

sections. If the curves in Figs. 6 and 7 are recast in this manner it is seen that on a plot of (σ_{max}/σ_y) against $(\sigma_y/\sigma_{cr})^{1/2}$ (Fig. 8), these quantities may be related by

$$\frac{\sigma_{max}}{\sigma_y} = \left(\frac{\sigma_{cr}}{\sigma_y}\right)^{0.54}.$$

Here

$$\sigma_{max} = \frac{P_{max}}{b_w h\left[1+2H\left(1-\frac{\alpha}{2}\right)+H_L(1-\alpha)\right]},$$

$$\sigma_{cr} = \frac{P_{cr}}{b_w h\left[1+2H\left(1-\frac{\alpha}{2}\right)+H_L(1-\alpha)\right]},$$

where H_L is the ratio of lip width to web width.

3. Experimental Investigation of Lipped Section Maximum Load

The special loading rig designed for this investigation is shown in Fig. 9. It consisted of two relatively massive plattens opposed to each other and individually mounted on four arms for vertical restraint and on two trunnions for restraint in the horizontal plane. The trunnions fitted over two heavy steel bars, one above the plattens and one below, which ran the length of the frame and were firmly attached to it. Rotation of the serrated hand wheels caused the end assemblies to approach each other thus inducing a load in the specimen channel, placed accurately in position in the grooved case-hardened face plates provided. Eccentric loading was obtained by the differential

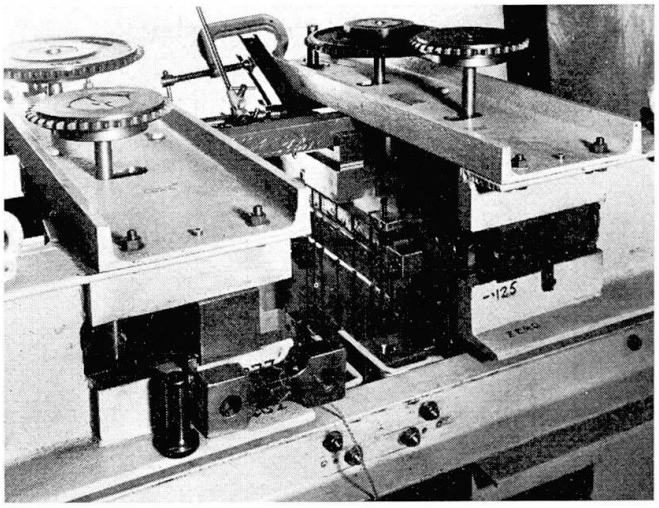

Fig. 9. View of experimental loading rig.

loading of one side from the other. The magnitude of the load was indicated by electrical resistance foil strain gauges bonded to the link bars and connected to a Huggenberger switch box and strain bridge. Each link bar was previously calibrated and was found to give a linear reading over the required load range. Collapse was indicated by a reduction of the load for an inward movement of the loading plattens. Results of this series of tests are plotted in Fig. 6 and 7.

Conclusions

An approximate method of analysis has been presented which assumes that a short channel column may be treated as a collection of individual plates connected appropriately along their common edges. The analysis combines the large deflection behaviour of these constituitive plates to provide an engineering estimate of the maximum load capacity of the channel.

The analysis is shown to give good predictions when applied to short columns subjected to eccentric loading. It is also found that the experimental results may be described adequately by a single curve relating the column theoretical buckling stress, the corresponding or maximum stress and the material yield stress. The test programme reported here was of limited range but the good agreement obtained promises hope for a coherent design formulation for open channel columns subjected to a variety of eccentric load actions.

Notation

a	plate, or channel, length.
b	plate breadth.
b_f, b_w	flange and web widths respectively of a channel section.
b_{01}, b_{11}, etc.	Galerkin coefficients in stress function series.

i, j, k, n	integers used in Galerkin deflection series.
k	buckling constant.
p, q, r, s	integers used in stress function series.
q_0, q_1, etc.	Galerkin coefficients in deflection function series.
r_1, r_0	degrees of rotational restraint per unit distance in x direction at plate edges $y=-b/2$ and $y=+b/2$ respectively.
t	plate thickness.
w	displacement of a point of the plate middle surface in a direction normal to the undeformed middle surface.
x, y	cartesian coordinates.
D	flexural stiffness of the plate, defined by $D=E\,t^3/12\,(1-\nu^2)$.
E	Young's modulus of the plate material.
F	Airy's stress function.
F'	non-dimensional form of Airy's stress function, $F'=F/E\,t^2$.
H	Channel shape factor, $H=b_f/b_w$.
H_L	ratio of lip width to flange width.
L	limit of deflection series.
N_x	normal force per unit length in the middle surface of the plate in the x direction.
N_0	value of N_x at $x=0$, $y=b/2$ and $x=a$, $y=b/2$.
N_0'	non-dimensional form of N_0, $N_0'=N_0\,a^2/\phi^2\,E\,t^2$.
N_{0cr}	critical value of N_0 at initial buckling.
P	total compressive load applied to plate.
P_{cr}	critical value of P at initial buckling.
P_{max}	maximum plate load.
T, U	limits of stress function series.
α	load eccentricity parameter.
κ_1, κ_0	non-dimensional forms of the degrees of rotational restraint per unit length in x direction at plate edges $y=-b/2$ and $y=+b/2$ respectively, $\kappa_1=-\frac{r_1\,b}{D}$, $\kappa_0=-\frac{r_0\,b}{D}$.
κ_f, κ_w	values of κ_1 at common edges for flange and web, respectively.
ν	Poisson's ratio of the plate material.
ξ, η	cartesian coordinates in non-dimensional form, $\xi=x/a$, $\eta=y/b$.
ϕ	aspect ratio of plate, $\phi=a/b$.
ϕ_f, ϕ_w	aspect ratio of flange and web, respectively, of a channel section.
σ_x, σ_y	direct stresses in the x and y direction, respectively.
σ_ξ, σ_η	non-dimensional forms of σ_x and σ_y, $\sigma_\xi=\frac{\sigma_x\,a^2}{\phi^2\,E\,t^2}$, $\sigma_\eta=\frac{\sigma_y\,a^2}{E\,t^2}$.
τ_{xy}	shearing stress in the $x\,y$ plane.
$\tau_{\xi\eta}$	non-dimensional form of τ_{xy}, $\tau_{\xi\eta}=\frac{\tau_{xy}\,a^2}{\phi^2\,E\,t}$.
ω	non-dimensional form of w, $\omega=w/t$.

References

1. GERARD, G.: Handbook of Structural Stability, Pt. IV Failure of Plates and Composite Elements, N.A.C.A., T.N. 3784, 1957.
2. CHILVER, A. H.: The stability and strength of thin-walled steel struts. The Engineer, p. 180, 1953.
3. CHILVER, A. H.: The maximum strength of the thin-walled channel strut. Civil Engineering, vol. 48, p. 1143, p. 1953.
4. WALKER, A. C.: Flat rectangular plates subjected to linearly-varying edge compressive loading. Thin walled Structures, Chatto and Windus, 1967.
5. WALKER, A. C.: Local stability in plates and channel struts. Journ. of the Struct. Div., Proc. A.S.C.E., vol. 92, No. ST 3, p. 39, 1966.
6. KARMAN, T. VON: Enzyklopädie der mathematischen Wissenschaften, vol. IV, p. 349, 1910.
7. PFLÜGER, A. VON: Thin walled compression members, Report No. 2, Institut für Statik der Technischen Hochschule Hannover, 1959.

Summary

An analytical and experimental investigation is made of the maximum load-carrying capacity of thin-walled open channel columns under eccentric compression. The channels are treated as being composed of individual plates connected appropriately along their common edges. The large deflection behaviour of these plates is analysed approximately using Galerkin's method and the results are synthesised to give an engineering estimate of the maximum load of the short columns.

The results of the experimental investigation show these estimates to be of good engineering accuracy and it is also shown that the results may be described adequately by a single curve relating the column buckling stress, the corresponding maximum stress and the material yield stress.

Résumé

Ce rapport présente une étude théorique et expérimentale sur la capacité de charge de piliers à section en U. On considère la section comme composée de parois individuelles, liées conformément. Les grandes déformations propres à ces plaques ont été analysées à l'aide de la méthode Galerkin. A partir des résultats obtenus, on réussit une estimation très générale de la capacité de charge de piliers courts, estimation qui se montre en bon accord avec les valeurs expérimentales. En plus on voit que les résultats peuvent être représentés par une seule courbe reliant la tension de flambage, la tension maximale correspondante et la limite d'écoulement du matériau.

Zusammenfassung

Es wird eine theoretische und experimentelle Studie über die Höchstlast dünnwandiger U-Stützen dargelegt. Man nimmt an, der Querschnitt sei aus einzelnen Platten zusammengesetzt, die an ihren Ecken entsprechend verbunden sind. Die diesen Platten eigenen großen Verformungen werden näherungsweise nach dem Galerkin-Verfahren untersucht. Die Synthese der Ergebnisse dient der praktischen Schätzung der Maximallast kurzer Stützen.

Die Versuchsergebnisse zeigen, daß diese Schätzung für praktische Zwecke genügend genau ist. Es wird ferner gezeigt, daß die Ergebnisse zweckmäßig durch eine einzige Kurve dargestellt werden können: Diese Kurve verbindet die Beulspannung, die entsprechende Maximalspannung und die Fließgrenze des Materials.

Leere Seite
Blank page
Page vide